THE JOURNAL OF PHYSICAL CHEMISTRY B

Article

pubs.acs.org/JPCB

Macromolecular and Morphological Evolution of Poly(styrene sulfonate) Complexes with Tetradecyltrimethylammonium Bromide

Alexey Popov,*[,†] Julia Zakharova,[†] Alexander Wasserman,[‡] Mikhail Motyakin,[‡] and Victor Kasaikin[†,§]

[†]Chemistry Department, Moscow State University, Moscow 119992, Russia

[‡]Semenov Institute of Chemical Physics, Russian Academy of Sciences, Moscow 119991, Russia

ABSTRACT: Macromolecular characteristics and morphology of water-soluble complexes between sodium poly(styrene sulfonate) (PSS) and tetradecyltrimethylammonium bromide have been followed as a function of surfactant-to-polymer charge ratio (S/P) to elicit possible changes in the complexation mechanism. As revealed by light scattering, shorter PSS (30 and 150 repeat units) yield multichain complexes while longer PSS (450 and 5000 repeat units) form single-chain species throughout $0 < S/P < 0.9$. Irrespective of PSS chain length, the complexes exist in solution in a swollen coil conformation and undergo a compaction with S/P but never collapse into a globule. Even when the free PSS chain is too short to coil (30 repeat units), the complexes adopt a coiled conformation due to multichain aggregation. Morphological changes (manifested by a hypochromic shift in UV spectra of the complexes at $S/P < 0.5$ and an increase in the local surfactant mobility observed at $S/P > 0.5$ by ESR) strongly suggest a change in the formation mechanism of the complexes with a transition near $S/P = 0.5$.

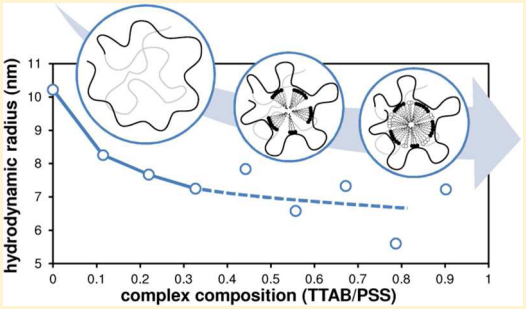

INTRODUCTION

Spontaneous formation of polymer−surfactant complexes (PSC) in aqueous mixtures of polyelectrolytes and oppositely charged surfactants represents a classical example of self-assembly.[1−3] This process is driven by electrostatic interactions between ionized groups of the polyelectrolyte and surfactant molecules and reinforced by aggregation of hydrophobic surfactant tails. As a result, binding in such systems follows the characteristic cooperative curve with little interaction at surfactant concentrations below the critical aggregation concentration (CAC) followed by a steep increase in the degree of binding over a small range of surfactant concentration once the CAC is surpassed. Subject to two counteracting tendencies—the tendency to maximize hydrophobic contact of the bound surfactant tails, on one hand, and the tendency to minimize entropy restrictions for the polymer chain, on the other—a PSC macromolecule in solution aims to achieve an equilibrium conformation that results in assembly of an intracomplex micellar phase (within one or a several polymer chains).[4−6] The morphology of such intracomplex micellar phases as well as overall PSC supramolecular organization depend strongly on the nature of PSC components. For example, PSC species can be comprised of either one (e.g., PSCs of polyacrylates and polymethacrylates) or multiple polyion chains (e.g., poly(diallyldimethylammonium chloride) with up to tens of chains per particle).[4,5] In the case of quaternized poly-4-vinylpyridine, either molecularly dispersed or aggregated PSCs are formed depending on the polymerization degree and complex composition.[6] Surfactant aggregation numbers in PSC micelles also vary in an extremely wide range depending on the components involved: from the numbers that are close to those in "free" micelles up to those that are orders of magnitude greater.[1−6]

Sodium poly(styrene sulfonate) (PSS) is widely employed in polymer-colloidal applications and commonly used in research as a model linear polyelectrolyte owing to the sulfonate functionality that ensures a high degree of ionization in water throughout the pH range.[7−12] However, complexation between PSS and oppositely charged surfactants exhibits a number of peculiar behaviors that can be presumably ascribed to the hydrophobic character of its benzene-based side groups.[13−21] One of the most distinct manifestations of such behaviors is the atypical shape of PSS−surfactant binding isotherms.[13,15−18] First of all, CACs observed in PSS solutions are several orders of magnitude lower than those observed with other conventional polyanions such as polyacrylates, poly(vinyl sulfate) (PVS), and dextran sulfate (DxS), suggesting an additional polymer−surfactant interaction in the case of PSS.[13,16−19,22,23] Second, PSS seems to display two distinct regimes of binding above the CAC: initial cooperative binding that is short-lived (unlike any other polyelectrolyte) and saturating at a binding degree of ∼0.5 followed by a noncooperative regime with a very slow increase in the amount of bound surfactant.[13,16−19] It should also be noted that, even in the cooperative regime, the cooperativity parameter exhibited by PSS is rather low in comparison to its nonaromatic counterparts. For example, the cooperativity parameter exhibited by PSS in binding tetradecyltrimethylammonium bromide in 20 mM NaCl is ∼70-fold

Received: May 17, 2012
Revised: August 7, 2012
Published: September 19, 2012

lower than that for PVS under the same conditions.[15,18] The low cooperativity of binding is consistent with formation of unusually small surfactant clusters (comprised of as few as 10−20 surfactant ions as determined by fluorescence quenching) in the case of PSS.[13−15,24] For comparison, surfactant aggregation numbers in complexes of PVS and DxS, as a rule, exceed 100.[22] Quaternized poly-4-vinylpyridine, perhaps the closest structural analogue of PSS among polycations, forms PCSs with surfactant clusters comprising a minimum of 600−800 surfactant ions.[6]

Another hallmark feature of PSS is an exceptionally wide solubility range of its PSCs. Generally, complexation between polyelectrolytes and oppositely charged surfactants leads to precipitation as a result of charge neutralization and increased hydrophobicity. With the majority of polyelectrolytes, the onset of precipitation occurs at the molar charge ratio of surfactant to polyelectrolyte in bulk (S/P) of ∼0.2−0.5.[19] Against conventional wisdom, complexes formed by PSS, a more hydrophobic polyelectrolyte, remain soluble even at S/P ratios as high as 0.7−1.[15,19,25] In a series of recent studies focused on complexes of PSS with alkylpyridinium surfactants, Kogej and co-workers attributed the wide solubility range to a less effective charge screening due to "a specific interaction between the hydrophobic benzene groups on the polyion and the surfactant micelles".[21] In agreement with this reasoning, their data on thermodynamic and transport properties of PSS−cetylpyridinium complexes in solution, including osmotic coefficient, enthalpy of dilution, and electrical conductivity, indicate that the fraction of free ions in the system is approximately the same up to 50% coverage of the polyion by surfactant ions but increases thereafter.[19] Such behavior suggests that the complexation results in formation of "trapped" thermodynamically inactive PSS−surfactant clusters below S/P = 0.5 but not beyond. Recently, this group also shed light on the conformation evolution of PSS PSC, additionally pointing to an inflection at around S/P = 0.5.[21] In particular, their results indicate that upon binding with cetylpyridinium chloride (CPC) chains of PSS (M_w = 1.52 × 10^5 and 2.26 × 10^6) undergo a strong compaction in the region between S/P = 0 and ∼0.5; further binding is, however, accompanied by a less pronounced (if any) compaction for the lower MW PSS or an expansion for the higher MW PSS. In conjunction with the strongly biphasic binding isotherms, the above data may be considered as evidence of a fundamental change in the PSC formation mechanism that occurs around S/P = 0.5 in the case of PSS. One may, however, reasonably argue that CPC is a somewhat exceptional surfactant itself due to its aromaticity and that its aromatic ring may be at least partially responsible for the specific interactions with the benzene group of the polyion (for example, due to aromatic stacking).

Much intrigued by the recent findings of Kogej and co-workers, we aimed to elicit the differences in PSS complexation with oppositely charged surfactants below and above S/P = 0.5 using a representative system unobscured by aromaticity of the surfactant. For this purpose, we investigated the evolution of macromolecular (molecular weight, size, and conformation) and morphological (local dynamics of the intracomplex micellar phase) characteristics of water-soluble PSCs formed in dilute solutions of PSS and tetradecyltrimethylammonium bromide, a nonaromatic medium-chain-length cationic surfactant, by means of light scattering and ESR spectroscopy.

EXPERIMENTAL SECTION

Materials. Sodium poly(styrene sulfonate)s PSS 30 and PSS 150 (weight average polymerization degrees P_w = 30 and 150, respectively) purchased from American Polymer Standards Corporation were used as received. PSS 450 (P_w = 450, Aldrich) and PSS 5K (P_w = 5000, Polysciences Corp.) were purified from low molecular weight contaminants by extensive dialysis against bidistilled water followed by lyophiliyzation. Water content in all PSS samples was quantified by TGA. The degree of sulfonation of no less than 97% was confirmed by elemental analysis. The weight average polymerization degrees were confirmed by small angle static light scattering. Tetradecyltrimethylammonium bromide, TTAB (Tokyo Casei, Inc.), and other materials were used as received.

PSCs were prepared via dropwise addition of a concentrated aqueous TTAB solution to 0.05−0.1 M PSS solutions in 50 mM NaBr at vigorous stirring to a desired surfactant-to-polyelectrolyte molar charge ratio, S/P = C_{TTAB}/C_{PSS}. The obtained mixtures were then diluted to a target PSS concentration (25 mM or lower) by addition of 50 mM NaBr and allowed to equilibrate for at least 12 h under gentle stirring at room temperature. All PSCs were prepared and tested in the presence of 50 mM NaBr.

Characterization Methods. Spectrophotometry was performed with a Hitachi 150-20 spectrophotometer. Relative absorbance A/A_0 was determined at λ_{max} in the 261−263 nm region. Prior to measurements, insoluble fractions (if any) were removed by centrifugation at 10 000 rpm.

Low angle static light scattering (SLS) and dynamic light scattering (DLS) experiments were performed using a Milton-Roy Chromatix KMX-6/DC small angle photometer (scattering angle θ = 6.5°) equipped with a 5 mW He−Ne laser (λ_0 = 630 nm, 5 mW). Multiangle SLS was performed on an "ALV-5" goniometer equipped with a 10 mW He−Ne laser (λ_0 = 630 nm). SLS data were processed according to the Zimm equation:

$$\frac{Kc}{R_\theta} = \frac{1}{M_w}(1 + 2A_2M_wc)\left(1 + \frac{R_g^3}{3}q^2\right) \quad (1)$$

where R_θ is the Rayleigh factor (measured by SLS), M_w is the weight average molecular weight, A_2 is the second virial coefficient, R_g is the radius of gyration, $q = (4\pi/\lambda)\sin(\theta/2)$ is the scattering vector, and K is the optical constant expressed as

$$K = \frac{4\pi^2n^2}{\lambda_0^4N_A}\left(\frac{dn}{dc}\right)^2 \quad (2)$$

where n is the medium refractive index, λ_0 is the laser wavelength in vacuum, N_A is the Avogadro number, and dn/dc is the refractive index increment (measured separately). For PSS 30, PSS 150, PSS 450, and their complexes, M_w values were calculated from low angle SLS data by extrapolating $Kc/R_{\theta=6.5}$ measured for a series of concentrations to c = 0. The error introduced by omitting extrapolation to zero angle did not exceed 5% of the M_w value as determined with polystyrene standards. For PSS 5K and its complexes, M_w and R_g values were calculated by extrapolating Kc/R_θ measured for a series of concentrations across multiple angles (θ = 30−150°) to zero concentration and zero angle (Zimm plot method). In all cases, Kc/R_θ vs c dependencies maintained linearity in the entire range tested, confirming that the scatterer's molecular weight was unaffected by the concentration (i.e., sample dilution did

dx.doi.org/10.1021/jp304819p | J. Phys. Chem. B 2012, 116, 12332−12340

not result in dissociation of the PSCs). Refractive index increments dn/dc were measured on a Milton-Roy Chromatix KMX-16 differential refractometer equipped with a He−Ne laser (λ_0 = 630 nm) operated at 2 mW. Reference solutions for dn/dc measurements were prepared by equilibrating the solvent (50 mM NaBr) against a respective PSC solution in a dialysis chamber in order to equalize concentrations of small molecule components in the reference and sample solutions.

In DLS experiments, autocorrelation functions of the scattered light intensity fluctuations were measured with a Langley-Ford Model 1096 Correlator and processed by the cumulants method to obtain the translational self-diffusion coefficient D_z. The hydrodynamic radus R_h was then calculated by extrapolating D_z to its value at zero concentration (D_0) and applying the Stokes−Einstein equation. In all cases, the hydrodynamic dimensions were unaffected by dilutions as confirmed by the linearity of the D_z vs c dependences in the range of concentrations tested. Prior to DLS/SLS measurements, all solutions were thoroughly prefiltered through 0.2 um pore size Millipore membranes.

The spin probe (structure shown in Scheme 1) was synthesized and kindly provided by A.B. Shapiro, Institute of Biochemical Physics, Russian Academy of Sciences. To introduce into the PSC, the spin probe was first dissolved in an aqueous solution of TTAB with the surfactant concentration above the critical micelle concentration at the probe to TTAB mole ratio of 1:50 or 1:100. A required amount of this stock solution was added to aqueous solutions of PSS during vigorous stirring and allowed to equilibrate with further stirring until complete dissolution. The obtained PSC solution was then mixed with additional TTAB (without the probe) if necessary. The probe concentration in the final samples was 0.05−0.2 mM. The electron paramagnetic resonance (EPR) spectra were recorded with a RADIOPAN (Poland) X-band spectrometer operating at a microwave frequency of 9.7 GHz with 100 kHz magnetic field modulation. The modulation amplitude was varied in the range 0.5−1.2 G, depending on the line width. The microwave power in the resonator did not exceed 3 mW in order to obviate the saturation effects. The rotational diffusion of the probes was calculated within the anisotropic Brownian motion model using the software described elsewhere.[26] The parameters used in this model are the coefficients of rotational diffusion around the axes, perpendicular ($R_\perp$) and parallel ($R_\parallel$) to the main axis of the molecule rotation, and the angle (β) between directions of the main axes of the diffusion tensor and the tensor of hyperfine (or Zeeman's) interactions. We assumed in our calculations a β value of 23° and the ratio of the rotational diffusion coefficients with respect to the different axes $n = R_\parallel/R_\perp = 2.5$.[27] The average correlation time τ is related to the rotational diffusion coefficient as follows: $\tau = 1/6R_{av}$, where $R_{av} = (R_\perp^2 \times R_\parallel)^{1/3}$. In calculating spectra, an important problem is the choice of the principal values of magnetic tensors of hyperfine and Zeeman's interactions. We used the following principal values of the g-tensor of radical: g_{xx} = 2.0095, g_{yy} = 2.0063, and g_{zz} =2.0022 and for the tensor of hyperfine interaction: A_{xx} = 7 G, A_{yy} = 5.2 G, and A_{zz} = 37 G.[27] During simulation, the hyperfine interaction tensor was varied within 0.5 G in order to attain the optimal fit between the experimental spectra and the theoretical values.

Scheme 1. Chemical Structure of the Spin Probe Used in the Study

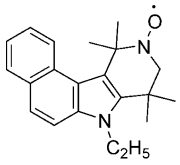

RESULTS AND DISCUSSION

Macromolecular Characteristics of PSS−TTAB Complexes. To investigate possible differences in the formation of PSS−TTAB complexes below and above S/P = 0.5, we first focus on the evolution of their macromolecular characteristics (weight, size, and conformation) against the degree of binding. Considering that prior data suggest an influence of PSS chain length on the structural properties of its complexes,[21] we have purposely decided to include in our investigation PSS samples with a wide range of polymerization degrees (P_w = 30, 150, 450, and 5000). To avoid crossing over into the semidilute regime where polymer chains start to overlap, we have chosen to operate at the maximum PSS concentration of 25 mM and with an added ionic strength of 50 mM. The added salt also served to suppress the polyelectrolyte swelling effect. As the first step of the investigation, it was necessary to confirm the solubility range in aqueous mixtures of PSS and TTAB in order to establish compositional boundaries for light scattering experiments. (Although PSS PSCs are generally known to have an extremely wide solubility range, the exact precipitation conditions found in the literature vary within S/P ≈ 0.7−1.0 depending on surfactant chemistry (alkyl chain length and the nature of the charged group)[15,20,21,25] and mixing conditions.[28]) For this purpose, we performed a precipitation study, in which PSS solutions were titrated with TTAB up to the mixture composition of S/P = 1.7. Obtained mixtures were centrifuged to remove any insoluble components, and the amount of PSS remaining in the supernatants was quantified by spectrophotometry. Relative absorbance curves for supernatants obtained from the mixtures of PSS 30 and PSS 450 are shown in Figure 1 as a representative example (similar results were observed for PSS 150 and PSS 5K).

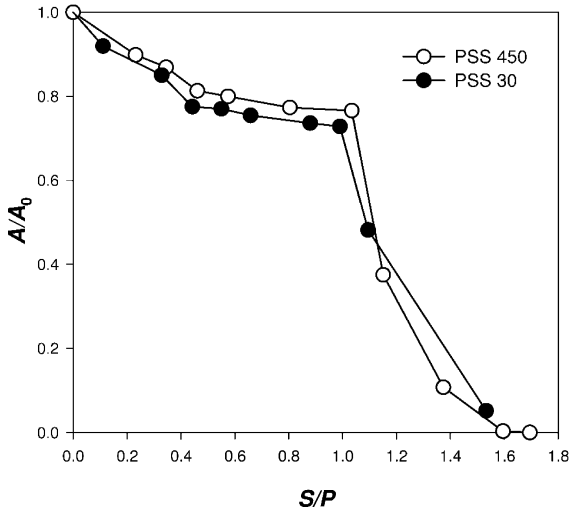

Figure 1. Relative absorbance of supernatants obtained from mixtures of PSS 30 and PSS 450 with TTAB: The sharp drop in A/A_0 at S/P ≈ 1 marks the onset of phase separation. C_{PSS} = 25 mM, 50 mM NaBr, 20 °C. Similar results were obtained for PSS 150 and PSS 5K.

dx.doi.org/10.1021/jp304819p | J. Phys. Chem. B 2012, 116, 12332−12340

As evident from Figure 1, increasing S/P from zero to 1 was accompanied by an approximately 25% decrease in absorbance followed by a sharp drop above the stoichiometric composition. Despite the measurable absorbance decrease below S/P ≈ 1, formation of insoluble complexes in this region was positively ruled out by visual monitoring of turbidity/precipitation (or, to be precise, lack thereof) in the mixtures before centrifugation. In fact, this initial decrease in A/A_0 appears to be due to a hypochromic shift caused by a rearrangement of PSS aromatic moieties as a result of PSS−surfactant binding. Although most known in conjunction with biomacromolecules and organic dyes, hypochromism has been observed in aqueous solutions of PSS as well, in particular, upon ionic strength addition or alteration of PSS stereochemistry.[29−32] The significance of this hypochromic shift with respect to the PCS structure will be specifically addressed later. As to the actual onset of phase separation in these systems, consistently with the gross figures from the literature, it occurs near the stoichiometric mixture composition as captured by the sharp drop in relative absorbance starting at S/P ∼ 1 and confirmed by the visual observation of turbidity/precipitation.

PSS−TTAB solutions obtained in the confirmed solubility region of 0 ≤ S/P ≤ 0.9 were examined by light scattering. The results of static light scattering measurements presented in Table 1 and Figure 2 indicate that increasing the S/P ratio was accompanied by a continuous increase in M_w for all four PSS fractions. Keeping in mind that CAC values for PSS−TTAB are on the order of 10^{-6} M under relevant conditions[16] and the total TTAB concentrations were greater than 2.5 mM in our experiments, the complex composition in the studied solutions can be essentially equated to the reaction mixture composition S/P with a correction only for the equilibrium surfactant concentration (i.e., <1% of the total TTAB concentration). Under this assumption, the average number of PSS chains (N) in a soluble PSC particle can then be calculated from the experimental M_w values following the reaction equation and mass-balance logic:

$$N = M_w/(P_w[M_{PSSNa} + S/P\cdot\{M_{TTAB} - M_{Na} - M_{Br}\}]) \quad (3)$$

where M_{PSSNa}, M_{TTAB}, M_{Na}, and M_{Br} are respectively molar masses of PSS monomer unit, TTAB, and the counterions released upon complexation (although it may be debated whether all counterions are released upon complexation, correcting for these considerations would yield essentially the same results as below even when assuming the fully unreleased case). The outcomes of eq 3 presented in Table 1 indicate that binding between TTAB and the lower molecular weight PSS samples (PSS 30 and PSS 150) led to intermolecular association of the polyions. The association is also illustrated by Figure 2, which shows that the experimental M_w (represented by round symbols) for these complexes increase faster than the values theoretically calculated assuming one PSS chain per complex particle (represented by lines 1 and 2). This association is most drastic in the case of PSS 30, the shortest PSS in the series—its PSCs aggregate up to nearly 5 polyions per particle. Keeping in mind that assembly of an intracomplex micellar phase is a necessary condition for PSC formation, we believe that the intermolecular association observed here of PSS 30 and PSS 150 is driven by the tendency to form an intracomplex micelle. In the case of these rather short chains, such a micelle apparently cannot be completed within a single chain likely due to the chain stiffness and/or insufficient numbers of bound surfactant ions even at the stoichiometry. On the other hand, the higher molecular weight PSS samples (PSS 450 and PSS 5K) form PSC particles comprised of a single polyelectrolyte chain in the entire range of their solubility, as shown in Table 1. The experimentally measured M_w for PSCs of PSS 450 and PSS 5K (square symbols in Figure 2) match the values calculated assuming one PSS chain per complex particle (lines 3 and 4 in Figure 2) remarkably well across the entire range of tested compositions. The existence of molecularly dispersed PSC in solutions of PSS 450 and PSS 5K is somewhat inconsistent with an observation by Kojeg et al. that PSS P_w ∼ 680 and P_w ∼ 12K form transient hydrophobically stabilized multichain aggregates upon complexation with CPC.[21] This difference can be attributed perhaps to the more hydrophobic nature of CPC (as compared to TTAB) and/or to specific interactions due to CPC's aromaticity that may lead to a stronger attraction between hydrophobic PSS−CPC clusters in aqueous media. Indeed, it has also been reported that binding of CPC induces a pronounced compaction of the PSS chains in the S/P ≤ 0.5 region, which can be interpreted as an intramolecular manifestation of strong hydrophobic interactions.[21]

To get an insight into the evolution size and conformation of PSS−TTAB complexes, we first exploited DLS as a relatively

Table 1. Weight Average Molecular Weight (M_w) and Number of PSS Chains (N) for PSS−TTAB Complexes (Measured by SLS and Calculated Using eq 3, Respectively)

PSS	S/P	M_w (kDa)	N
PSS 30	0.00	6	1.0
	0.11	23	3.3
	0.22	27	3.5
	0.33	24	2.9
	0.44	40	4.3
	0.55	34	3.4
	0.66	52	4.8
	0.77	46	3.9
	0.88	55	4.5
PSS 150	0.00	31	1.0
	0.10	45	1.3
	0.20	50	1.3
	0.30	50	1.2
	0.40	70	1.5
	0.50	62	1.3
	0.60	96	1.8
	0.70	93	1.7
	0.80	85	1.4
PSS 450	0.00	92	1.0
	0.12	106	1.0
	0.22	112	1.0
	0.33	120	1.0
	0.44	143	1.0
	0.56	148	1.0
	0.67	172	1.1
	0.79	173	1.0
	0.90	226	1.2
PSS 5K	0.00	1034	1.0
	0.10	1230	1.1
	0.25	1560	1.2
	0.40	1630	1.1
	0.50	1627	1.0
	0.75	2200	1.2

dx.doi.org/10.1021/jp304819p | J. Phys. Chem. B 2012, 116, 12332−12340

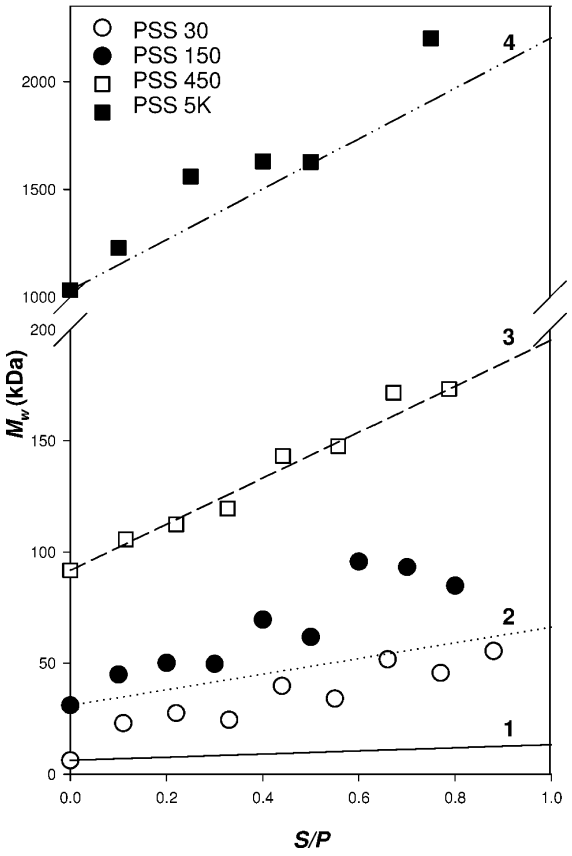

Figure 2. Dependence of the weight average molecular weight, M_w, on the S/P ratio in solutions of PSS 30, PSS 150, PSS 450, and PSS 5K. Symbols represent measured M_w values. Lines 1, 2, 3, and 4 represent M_w values calculated assuming one PSS chain per complex particle for PSS 30, PSS 150, PSS 450, and PSS 5K, respectively.

simple technique for hydrodynamic size characterization. As illustrated in Figure 3, addition of surfactant ions onto PSS chains did not increase their overall hydrodynamic size despite the continuously increasing M_w. An exception from this observation should be made for PSCs of PSS 30 and PSS 150 at S/P = 0.1 that showed hydrodynamic radius (R_h) values higher than those for the free chains. A likely explanation for this increase is the interchain aggregation induced by surfactant binding to these shorter polyions (discussed previously in the context of the SLS results). Remarkably, the hydrodynamic size of these PCSs did not continue increasing past S/P = 0.1 and, in fact, dropped immediately after S/P = 0.1 even though greater N values were observed for these PSCs at higher binding degrees (Table 1). This behavior can be tentatively ascribed to a significant compaction of the chains. However, the multichain character of these PSCs and their somewhat fluctuating aggregation numbers to an uncertain extent obscure interpretation of these R_h trends. In this respect, single-chain PSCs formed by PSS 450 and PSS 5K are more telling. As shown in Figure 3, binding of TTAB to PSS 450 and PSS 5K was clearly accompanied by a decrease of R_h for both chains. In the case of PSS 450, the decrease was perhaps most pronounced in the S/P $\leq$ 0.4 region, suggesting a possible change in the complex formation around S/P = 0.5. However, progressively high fluctuations of R_h above S/P = 0.4 compromise clarity of the trend. Moreover, the R_h decrease appears to be monotonous across the entire S/P range, without a hint of a major change near S/P = 0.5, in the case of PSS 5K. It should be noted though that, with R_h being a dynamic characteristic, interpretation of its changes is inherently ambiguous: decreasing R_h may be explained by either a true compaction (e.g., compaction of a swollen coil to a denser coil) or a shape change (e.g., transition from rod-like to spherical shape). An obvious approach to resolving this ambiguity is predicated on parallel monitoring of a static size characteristic, i.e., the radius of gyration R_g. The ratio of R_g/R_h is known to reflect the shape of a particle as follows: R_g/R_h = 0.77, ~1.8, and >2 for a solid sphere, coil, and rigid rod-like chain, respectively. Therefore, we attempted to measure R_g for PSS 450, PSS 5K, and their PSC by using the Zimm plot method. Unfortunately, this approach failed for PSS 450 and its complexes due to a low angular dependency of their scattered intensity. However, the Zimm plot method worked well for the larger particles of PSS 5K. The values of R_g successfully obtained for PSS 5K and its complexes together with their respective R_g/R_h ratios are presented in Table 2. In the entire

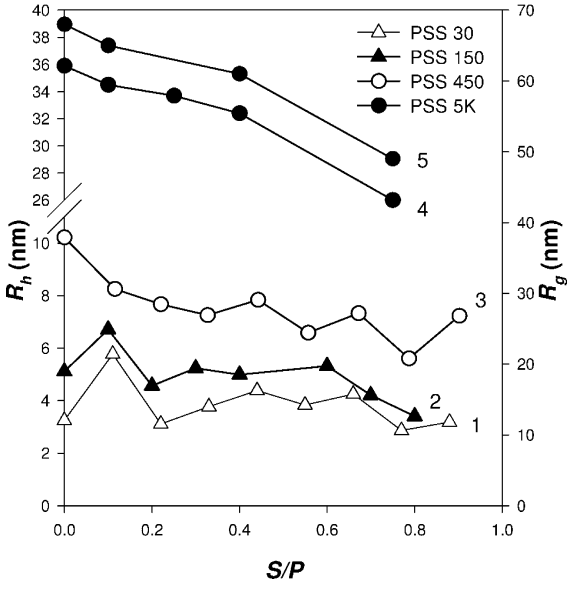

Figure 3. Hydrodynamic radii R_h of PSS 30, PSS 150, PSS 450, PSS 5K, and their complexes with TTAB (left scale, curves 1, 2, 3, 4). Additionally presented are radius of gyration R_g values for PSS 5K and its complexes (right scale, curve 5).

Table 2. Size Characteristics of PSS 5K and Its Complexes with TTAB

S/P	R_h (nm)	R_g (nm)	R_g/R_h
0	35.9	68	1.89
0.1	34.5	65	1.88
0.4	32.4	61	1.88
0.75	26.0	49	1.88

range of 0 $\leq$ S/P $\leq$ 0.75, the R_g/R_h ratio remained constant at a value of ~1.9, which is indicative of a swollen coil conformation. Therefore, it can be concluded that binding of TTAB to PSS 5K resulted in a true compaction of coil-shaped chains (but not to the extent of collapsing into a globular conformation).

To further elucidate the conformation of PSS–TTAB complexes, we exploited the scaling relationship between D_0 and M_w that is based on the Mark–Houwinck equation:

dx.doi.org/10.1021/jp304819p | J. Phys. Chem. B 2012, 116, 12332–12340

$$D_0 \propto M^{-a} \quad (4)$$

where α is a conformational parameter describing the compactness of the chain in solution: 0.33 for a compact sphere, 0.5 for an ideal coil, 0.6 for a coil in good solvent, and 1 for a rigid rod. Shown in Figure 4 is a log–log plot of

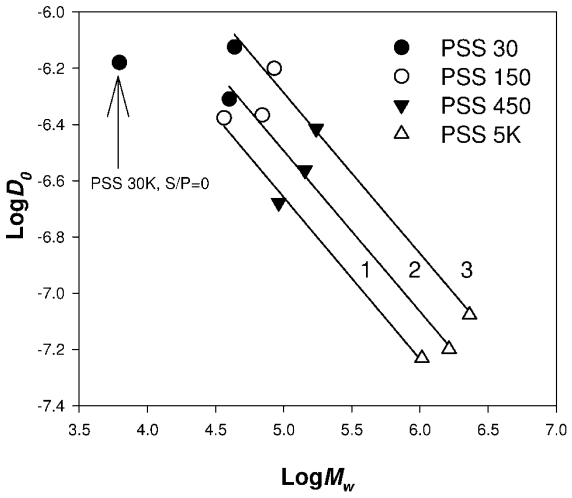

Figure 4. Log–log plot of experimentally measured D_0 vs M_w for PSCs formed by PSS 30, 150, 450, and 5K and TTAB at S/P ratios of 0, 0.4, and 0.8. The lines show results of a linear fit across the four PSS fractions at a given S/P ratio: (1) S/P = 0, $y = -0.58x - 3.78$, $R^2 = 0.99$ (fit performed excluding the data-point for PSS 30); (2) S/P = 0.4, $y = -0.57x - 3.43$, $R^2 = 0.99$; (3) S/P = 0.8, $y = -0.57x - 3.64$, $R^2 = 0.99$.

experimentally measured D_0 vs M_w for PSS 30, 150, 450, and 5K and their PSCs with TTAB at S/P ratios of 0.4 and 0.8. Each of the lines in Figure 4 represents an extrapolation across the four PSS fractions at a given S/P (i.e., the source of increased M_w along each extrapolation is the increase in length of the polymer chain form 30 to 5000 units, not the addition of surfactant ions). All four extrapolations resulted in linear fits (except the data point corresponding to PSS 30 at S/P = 0), and they all have the same slope of ~0.6 characteristic for a coil in a good solvent. Therefore, it can be concluded that the conformation of these PSS chains remained globally unchanged as the degree of binding progressed from 0 to 0.4 to 0.8. Keeping in mind the observed R_h decrease, this result confirms a true compaction of PSS 5K and suggests the same compaction (rather than a shape change) for PSS 450 and PSS 150. As for PSS 30, diffusion of its free chain deviates from the linear log D_0 vs log M_w dependence exhibited by the higher PSS fractions (line 1 in Figure 4). This deviation is likely due to the inability of such a short chain to realize a coil conformation. Indeed, the length of a fully stretched PSS 30 chain is ~7 nm, while the persistence length of PSS under the experimental conditions is ~4.5 nm (estimated from the data of Nishida[33] using the total ionic strength calculated according to the condensation theory of Oosawa–Manning as $I = [0.35C_{PSS}/2 + C_{NaBr}]$, i.e., ~55 mM in our case). Remarkably, complexes of PSS 30 with TTAB exist in solution in a swollen coil conformation as evident from their excellent fit onto lines 2 (S/P = 0.4) and 3 (S/P = 0.8) in Figure 4. This conformational transition can be attributed to formation of a "longer" macromolecule as a result of the interchain aggregation that occurs upon complexation of PSS 30 with TTAB and also to the reduction of the electrostatic persistence length due to charge neutralization.

In summary, our light scattering experiments have shown that, regardless of the chain length of the parent PSS molecule, all tested PSS–TTAB complexes exist in solution in a swollen coil conformation. Whether they are single-chain particles or multichain aggregates, the PSCs undergo a pronounced compaction as the binding degree increases but maintain a coiled conformation at least up to S/P = 0.8. Hence, two conclusions follow: (1) Although the R_h trend for PSS 450 shows a greater magnitude of change due to chain compaction below S/P = 0.5 followed by a less pronounced change at higher complex compositions, there is no strong overall evidence of a mechanistic change in PSS–TTAB complexation near S/P = 0.5 based solely on the evolution of their conformation and size. (2) All four PSS chain lengths tested here produced PSCs that are conformationally isostructural (swollen coils), and any of these PSS samples may be used in the further investigation of the intracomplex morphology; PSS 450 and PSS 5K may be preferred due to the less ambiguous single chain character of their PSC species.

Morphology of PSS–TTAB Complexes. To elucidate the evolution of internal morphology of PSS–TTAB complexes, we tested water-soluble PSCs formed by PSS 450 as a representative sample, by means of UV spectrophotometry and ESR. As shown in Figure 5, binding of TTAB to the

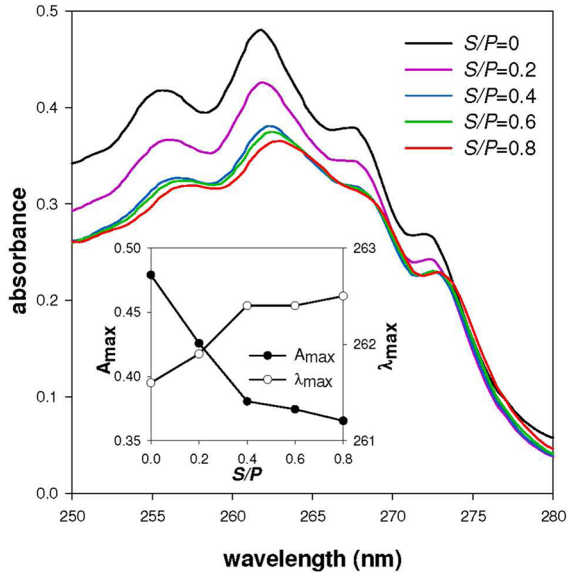

Figure 5. UV absorbance spectra of PSS 450 and its complexes with TTAB in aqueous solution (C_{PSS} = 12.5 mM, 0.1 mm optical path). The inset shows the wavelength (λ_{max}) and magnitude (A_{max}) of absorbance maxima.

polyion up to S/P ~ 0.4 was accompanied by hypochromic (absorption reduction) and bathochromic (increase of λ_{max}) shifts in UV spectra of PSS. Hypochromicity is expected when chromophores become stacked on each other under conditions where the electrostatic potential between them is decreased.[30,34,35] For example, hypochromic shifts have been observed in aqueous PSS solutions upon increasing ionic strength or upon alteration of PSS stereochemistry from atactic or syndyotactic to isotactic.[29−32] Since in the case of PSS–TTAB complexes an excess of salt (50 mM NaBr) was present in all test solutions to suppress local ionic strength fluctuations,

dx.doi.org/10.1021/jp304819p | J. Phys. Chem. B 2012, 116, 12332–12340

the observed hypochromicity is likely due to a rearrangement of the PSS side groups into more tightly packed (possibly stacked) clusters as bound surfactant ions neutralize their charges and "pull" them into the micellar phase. Indeed, stacking of PSS benzene rings and/or their incorporation into the micellar phase have been previously suggested by NMR studies.[36,37] Since the observed hypochromic and bathochromic shifts appear to plateau at S/P ∼ 0.4, it can be suggested that the number of the side groups involved in such clusters is limited to ∼40% of the entire chain and that further binding of TTAB to PSS is not accompanied by a significant rearrangement/clusterization of the side groups.

The spin probe technique has been previously shown to characterize the molecular organization and dynamics of the micellar phase of PSC.[38,39] A spin probe rotation correlation time (τ) is a function of the molecular mobility and packing density of the surrounding surfactant ions. Figure 6 displays ESR spectra of the spin probe solubilized by free TTAB micelles as well as TTAB−PSS complexes. The values of τ deduced from these spectra point to a significant reduction in the local mobility of the PSS-bound micellar phase upon the initial stage of complexation (0 < S/P < 0.6), as demonstrated by the 6-fold increase of τ relative to the free micelles (Figure 7). Further binding is, however, accompanied by a continuous decrease of τ all the way up to the onset of phase separation,

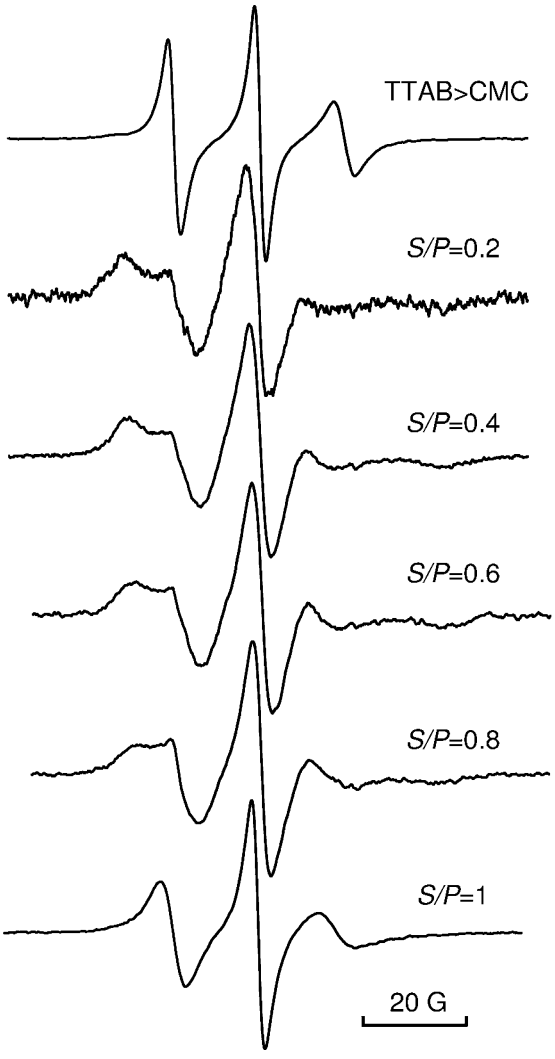

Figure 6. ESR spectra of the spin probe in free TTAB micelles and TTAB−PSS complexes.

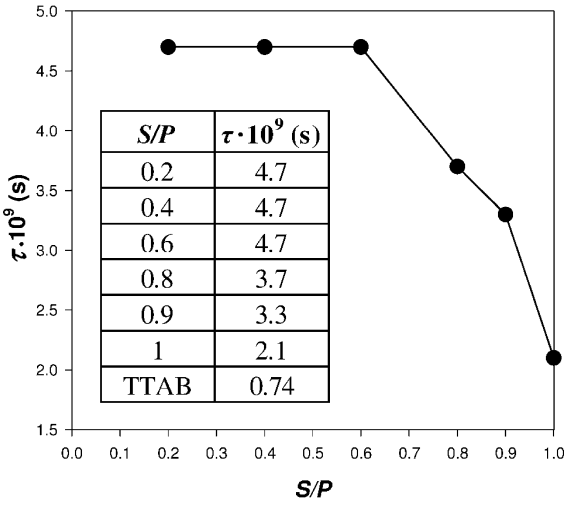

Figure 7. Correlation times (τ) for the spin probe solubilized by TTAB micelles and PSS−TTAB complexes.

indicating a continuous increase in the average local mobility of the bound surfactant ions above S/P = 0.6 and up to the formation of insoluble PSC. This, in turn, suggests a change in the mechanism of binding between the surfactant and polyion that occurs at S/P ∼ 0.6. Such a change may involve a reassembly or transformation of the existing micellar phase into a less rigid structure (e.g., from multiple small and rigid spherical micelles into one larger and more fluid micelle) or a "loosening" of the micellar phase by adding a new component, one less organized and more mobile than that formed at S/P < 0.6 (e.g., by forming new, less rigid micelles or by completing the existing micelles with less tightly bound surfactant ions). The latter appears to be a more likely scenario for PSS−TTAB, considering that the hypochromic changes reach a plateau at S/P ∼ 0.4 but do not revert. On the other hand, more consistently with the "transformation" scenario, Nause et al. showed that spherical micelles formed by water-soluble complexes of PSS with cetyltrimethylammonium bromide at S/P ratios less than 0.5 coalesce into a single cylindrical micelle at S/P ≥ 0.5.[25] In any case, such a drastic alteration of the micellar phase morphology with complex composition within the soluble domain appears to be unique to PSS as it has not been observed with other PSC systems, including those previously studied by the spin probe method such as complexes of poly(acrylic acid), poly(methacrylic acid) and poly(dimethyldiallylammonium chloride).[38,39] Taken together, our UV and ESR spectroscopy findings strongly suggest the existence of two distinct stages of TTAB binding to PSS with a transition near S/P ∼ 0.5.

CONCLUSIONS

The evolution of macromolecular characteristics and intracomplex morphology of water-soluble PSS−TTAB complexes obtained in dilute aqueous solutions has been followed as a function of surfactant-to-polymer ratio (S/P) by means of light scattering, UV spectrophotometry, and ESR spectroscopy. We have shown that, regardless of the chain length of the parent PSS (from 30 to 5000 repeat units), the complexes exist in solution as swollen coils. Remarkably, the complexes adapt a

dx.doi.org/10.1021/jp304819p | J. Phys. Chem. B 2012, 116, 12332−12340

coiled conformation even when the parent polymer is too short to coil by itself as observed with PSS 30. Such a conformational transition upon complexation can be attributed to formation of a "longer" macromolecule as a result of an interchain aggregation, which is apparently driven by the need to assemble an intracomplex micellar phase. Whether they are single-chain species formed by PSS 450 and PSS 5K or multichain aggregates formed by PSS 30 and PSS 150, the complex macromolecules undergo a pronounced compaction as the degree of binding increases but maintain a coiled conformation in the entire range of their solubility. Overall, we found no sufficient evidence for a mechanistic change in PSS−TTAB complexation at S/P ≈ 0.5 based on the evolution of their conformation and size. However, a progressive hypochromic effect observed in UV spectra of the complexes below S/P ≈ 0.5 and an increase in the spin probe mobility observed above S/P ≈ 0.5 strongly suggest the existence of two distinct stages of TTAB binding to PSS with a transition near S/P ≈ 0.5. Ordinarily, the binding of ionic surfactants to polyelectrolytes of opposite charge is driven by electrostatic attraction of the two components and stabilized by hydrophobic association of the surfactant tails between themselves.[1−3] On the basis of our UV and ESR findings, we believe that in the case of PSS the initial binding (up to S/P ≈ 0.5) is additionally reinforced by stacking and/or inclusion of PSS benzene rings into the micellar phase. This hypothesis is consistent with extremely low CAC values generally exhibited by PSS and supports the argument of "a specific interaction between the hydrophobic benzene groups on the polyion and the surfactant micelles" proposed by Kogej and co-workers.[21,40] Furthermore, we believe that incorporation of the benzene groups that are covalently linked to the polyelectrolyte chain into the micellar phase hinders the lateral diffusion of surfactant ions (a behavior consistent with the reduced spin probe mobility at low S/P). This, in turn, may lead to formation of isolated hydrophobic clusters populated along the chain, as schematically illustrated in Figure 8. (The simplified depiction in Figure 8 is intended

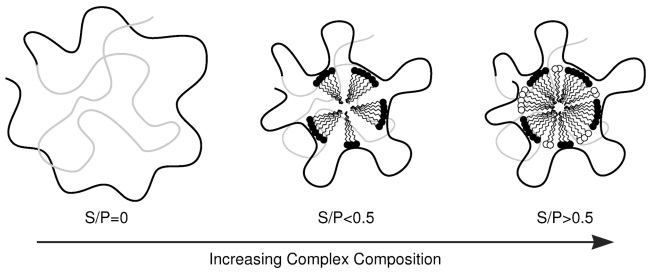

Figure 8. Schematic depiction of PSC evolution in PSS−TTAB solutions. Solid "heads" represent surfactant clusters reinforced by a specific interaction with PSS benzene rings. Open "heads" represent surfactant ions adhered to the complex without intimate bonds with PSS (not drawn to scale).

not to reflect all structural aspects of the complex, e.g., the micellar phase geometry, but to highlight the impact of localized surfactant clusters on the complex dimensions and micellar phase mobility as demonstrated in our experiments.) Indeed, the existence of small surfactant clusters (as small as 10 ions) in PSS−surfactant complexes was previously observed by others.[13−15,24] To maximize the hydrophobic contact, such "isolated" clusters must aggregate, causing the macromolecule to contract as demonstrated by light scattering here and elsewhere.[21] On the basis of the increased lateral mobility of surfactant ions as measured by the spin probe method above S/P ≈ 0.5 and the plateauing of the hypochromic shift above S/P ≈ 0.5, we believe that additional surfactant ions bind to the complex without forming the reinforced clusters. For example, it is possible that not all segments of PSS can form such reinforced clusters due to local configuration or conformation restrictions. It may also be possible that the chain compaction in the low S/P region forces unreacted portions of the polyelectrolyte into kinks/loops that become spatially less available for further inclusion into the micellar phase. Thus, additional surfactant ions may bind to the complex without forming intimate bonds with the unreacted polyelectrolyte units (for example, by adhering to the already existing micellar phase via hydrophobic forces). As a result, the PSC macromolecule behaves essentially as a zwitterion bearing both negative and positive charges above S/P ∼ 0.5, which may explain the hallmark behavior of PSS complexes—aqueous solubility even near the stoichiometric 1:1 composition.

AUTHOR INFORMATION

Corresponding Author

*Present address: Kala Pharmaceuticals, 135 Beaver Street, Waltham, MA 02453, USA. E-mail: alexey.popov@kalarx.com.

Notes

The authors declare no competing financial interest.

[§]Deceased.

REFERENCES

(1) Goddard, E. D. *Colloids Surf.* **1986**, *19*, 301−329.
(2) Goddard, E. D.; Ananthapadmanabhan, K. P. *Interactions of surfactants with polymers and proteins*; CRC Press: Boca Raton, FL, 1993.
(3) Bain, C. D.; Claesson, P. M.; Langevin, D.; Meszaros, R.; Nylander, T.; Stubenrauch, C.; Titmuss, S.; von Klitzing, R. *Adv. Colloid Interface Sci.* **2010**, *155*, 32−49.
(4) Ibragimova, Z. K.; Ivleva, Y. M.; Pavlova, N. V.; Borodulina, T. A.; Yefremov, V. A.; Kasaikin, V. A.; Zezin, A. B.; Kabanov, V. A. *Polym. Sci.* **1992**, *34*, 808−812.
(5) Kabanov, V. A.; Zezin, A. B.; Kasaikin, V. A.; Zakharova, J. A.; Litmanovich, E. A.; Ivleva, E. M. *Polym. Int.* **2003**, *52*, 1566−1572.
(6) Zakharova, J. A.; Otdelnova, M. V.; Ivleva, E. M.; Kasaikin, V. A.; Zezin, A. B.; Kabanov, V. A. *Polymer* **2007**, *48*, 220−228.
(7) Petzold, G.; Schwarz, S. *Sep. Purif. Technol.* **2006**, *51*, 318−324.
(8) Hoagland, D. A.; Arvanitidou, E.; Welch, C. *Macromolecules* **1999**, *32*, 6180−6190.
(9) Izumrudov, V. A.; Volkova, I. F.; Grigoryan, E. S.; Gorshkova, M. Y. *Polym. Sci., Ser. A* **2011**, *53*, 281−288.
(10) Radeva, T. *Physical chemistry of polyelectrolytes*; Marcel Dekker: New York, 2001.
(11) Sehgal, A.; Seery, T. A. P. *Macromolecules* **1998**, *31*, 7340−7346.
(12) Zhang, B.; Hattori, T.; Dubin, P. L. *Macromolecules* **2001**, *34*, 6790−6794.
(13) Almgren, M.; Hansson, P.; Mukhtar, E.; Vanstam, J. *Langmuir* **1992**, *8*, 2405−2412.
(14) Andersson, M.; Rasmark, P. J.; Elvingson, C.; Hansson, P. *Langmuir* **2005**, *21*, 3773−3781.
(15) Hansson, P.; Almgren, M. *Langmuir* **1994**, *10*, 2115−2124.
(16) Hayakawa, K.; Kwak, J. C. T. *J. Phys. Chem.* **1982**, *86*, 3866−3870.
(17) Hayakawa, K.; Kwak, J. C. T. *J. Phys. Chem.* **1983**, *87*, 506−509.
(18) Hayakawa, K.; Shinohara, S.; Sasawaki, S.; Satake, I.; Kwak, J. C. T. *Bull. Chem. Soc. Jpn.* **1995**, *68*, 2179−2185.
(19) Kogej, K. *Adv. Colloid Interface Sci.* **2010**, *158*, 68−83.
(20) Kogej, K.; Evmenenko, G.; Theunissen, E.; Berghmans, H.; Reynaers, H. *Langmuir* **2001**, *17*, 3175−3184.

(21) Prelesnik, S.; Larin, S.; Aseyev, V.; Tenhu, H.; Kogej, K. *J. Phys. Chem. B* **2011**, *115*, 3793−3803.
(22) Hansson, P.; Almgren, M. *J. Phys. Chem.* **1995**, *99*, 16694−16703.
(23) Shirahama, K.; Tashiro, M. *Bull. Chem. Soc. Jpn.* **1984**, *57*, 377−380.
(24) Abuin, E. B.; Scaiano, J. C. *J. Am. Chem. Soc.* **1984**, *106*, 6274−6283.
(25) Nause, R. G.; Hoagland, D. A.; Strey, H. H. *Macromolecules* **2008**, *41*, 4012−4019.
(26) Budil, D. E.; Lee, S.; Saxena, S.; Freed, J. H. *J. Magn. Reson., Ser. A* **1996**, *120*, 155−189.
(27) Wasserman, A. M.; Otdelnova, M. V.; Zakharova, J. A.; Aliev, I. I.; Motyakin, M. V.; Timofeev, V. P.; Kasaikin, V. A. *Chim. Fiz.* **2005**, 29−37 (in Russian).
(28) Pojjak, K.; Bertalanits, E.; Meszaros, R. *Langmuir* **2011**, *27*, 9139−9147.
(29) Aylward, N. N. *J. Polym. Sci., Part A: Polym. Chem.* **1970**, *8*, 909−916.
(30) Aylward, N. N. *J. Polym. Sci., Part A: Polym. Chem.* **1975**, *13*, 373−382.
(31) Aylward, N. N. *J. Polym. Sci., Part A: Polym. Chem.* **1977**, *15*, 231−241.
(32) Carroll, W. R.; Eisenber., H. *J. Polym. Sci., Part B: Polym. Phys.* **1966**, *4*, 599−610.
(33) Nishida, K.; Urakawa, H.; Kaji, K.; Gabrys, B.; Higgins, J. S. *Polymer* **1997**, *38*, 6083−6085.
(34) Itaya, T.; Ochiai, H.; Ueda, K.; Imamura, A. *Macromolecules* **1993**, *26*, 6021−6026.
(35) Kubota, M.; Ono, A. *Tetrahedron Lett.* **2004**, *45*, 1187−1190.
(36) Gao, Z.; Wasylishen, R. E.; Kwak, J. C. T. *J. Phys. Chem.* **1990**, *94*, 773−776.
(37) McLachlan, A. A.; Marangoni, D. G. *Can. J. Chem.* **2010**, *88*, 124−134.
(38) Kasaikin, V. A.; Wasserman, A. M.; Zakharova, J. A.; Motyakin, M. V.; Kolbanovskly, A. D. *Colloids Surf., A* **1999**, *147*, 169−178.
(39) Wasserman, A. M.; Kasaikin, V. A.; Zakharova, Y. A.; Aliev, I. I.; Baranovsky, V. Y.; Doseva, V.; Yasina, L. L. *Spectrochim. Acta, Part A* **2002**, *58*, 1241−1255.
(40) Sitar, S.; Goderis, B.; Hansson, P.; Kogej, K. *J. Phys. Chem. B* **2012**, *116*, 4634−4645.